ARTICLE

Observation-based selection of climate models projects Arctic ice-free summers around 2035

David Docquier [1✉] & Torben Koenigk[1,2]

Arctic sea ice has been retreating at an accelerating pace over the past decades. Model projections show that the Arctic Ocean could be almost ice free in summer by the middle of this century. However, the uncertainties related to these projections are relatively large. Here we use 33 global climate models from the Coupled Model Intercomparison Project 6 (CMIP6) and select models that best capture the observed Arctic sea-ice area and volume and northward ocean heat transport to refine model projections of Arctic sea ice. This model selection leads to lower Arctic sea-ice area and volume relative to the multi-model mean without model selection and summer ice-free conditions could occur as early as around 2035. These results highlight a potential underestimation of future Arctic sea-ice loss when including all CMIP6 models.

[1] Swedish Meteorological and Hydrological Institute, Rossby Centre, Norrköping, Sweden. [2] Bolin Centre for Climate Research, Stockholm University, Stockholm, Sweden. ✉email: docquier.david@gmail.com

The retreat of Arctic sea ice is one of the most striking consequences of global warming and has strong implications for local and remote climate, biosphere and society[1]. The total area of the Arctic Ocean covered by sea ice, the Arctic sea-ice area, has decreased by about 2 million km^2 (yearly average) in the past 40 years of satellite observations, with more pronounced loss in the summer[1–3]. As sea ice has also thinned by 1.5–2 m in the central Arctic since 1980[4,5], the total Arctic sea-ice volume has substantially decreased at a rate of about 3000 km^3 per decade since 1979[6,7]. The current Arctic sea-ice losses are strongly connected to rising global temperatures[8–10], and thus to cumulative greenhouse gas emissions into the atmosphere[3,11]. The observed sensitivity of sea-ice changes to cumulative greenhouse gas emissions has been used to provide an estimate of the future Arctic sea-ice area[11]. However, this simple linear extrapolation neglects non-linearities in the climate system and ocean-ice-atmosphere interactions and feedbacks[12–14], resulting in large short- and long-term deviations from the ongoing negative trend in sea-ice area and volume[15–18].

In order to include these non-linearities and interactions, climate models can be used to provide more reliable projections of the fate of Arctic sea ice[19,20]. In particular, global climate models coupling the atmosphere, ocean and sea ice are well suited to make such projections[21–24]. The inclusion of these models in the different Coupled Model Intercomparison Project (CMIP) phases[25–27] allows for estimates of Arctic sea-ice area and volume projections in the next decades to centuries. The latest CMIP6 modelling effort[27] will feed into the next Intergovernmental Panel on Climate Change Assessment Report 6 and includes climate model projections that follow different future greenhouse gas emission scenarios using the Shared Socioeconomic Pathways (SSPs)[28].

Our study is the first one, to the best of our knowledge, to make use of a large range of selection criteria to refine future projections of Arctic sea ice coming from the CMIP6 model simulations. We select models that best represent the present Arctic sea-ice state and northward ocean heat transport, as the latter is a major driver of recent sea-ice loss[29,30]. We find that the sea-ice loss over this century is larger using different model selection criteria compared to the average over all models without model selection. In particular, we find that summer ice-free Arctic conditions could occur as early as around 2035 in the selection case, compared to 2061 in the no-selection case.

Results and discussion

Projections without model selection. In our study, we focus on both the high-emission SSP5-8.5 and low-emission SSP1-2.6 scenarios, which correspond to a global warming of around 4 and 1 °C, respectively, over this century (2081–2100 relative to 1995–2014)[31]. Averaged over 33 CMIP6 models (totalling 166 model members, Supplementary Table 1), the multi-model mean March Arctic sea-ice area and volume are reduced by 45% and 78%, respectively, in 2096–2100, compared to 2015–2019, in the high-emission scenario (Fig. 1a and Supplementary Fig. 1a). In September, the multi-model mean Arctic sea-ice area and volume are decreased by 90% and 98%, respectively, at the end of the century (Fig. 1b and Supplementary Fig. 1b). In addition, the Arctic Ocean becomes almost ice free (sea-ice area lower than 1 million km^2 [14]) in September in 2061 for the multi-model mean, with a large inter-model spread covering the whole twenty-first century (Fig. 1b). Note that first ice-free conditions are reached about 10 years earlier (for the multi-model mean) in a previous CMIP6 study[24] that did not include two models that have a high mean state bias (which we include here) and used only the first member of each model.

These Arctic sea-ice area and volume changes are considerably slowed down in the low-emission scenario: the multi-model mean March sea-ice area and volume are reduced by only 8% and 28%, respectively, at the end of the century, while the September sea-ice area is decreased by 49% and thus never reaches almost ice-free conditions during this century, and the September sea-ice volume is lowered by 69% (Supplementary Figs. 2 and 3). However, model projections suffer from large uncertainties related to the chosen greenhouse gas emission scenarios, model physics and internal variability[32,33], such that the spread in future Arctic sea-ice projections is relatively large among climate models (Fig. 1 and Supplementary Fig. 2)[21,24]. In the high-emission scenario, the model spread increases over time for March sea-ice area (Fig. 1a), while it decreases for September sea-ice area as a large number of models lose almost all their sea ice around 2050 (Fig. 1b). In the low-emission scenario, the model spread in March and September sea-ice area does not substantially vary over time as the changes over the twenty-first century are not as large as in the high-emission scenario (Supplementary Fig. 2).

Model selection. Considering the simple average of all available models assumes that all models are equally plausible and that the range of their projections is representative of the uncertainty[34]. As some models better represent one specific aspect of the observed climate (Arctic sea ice in our case), we can argue that these models provide more accurate projections of this specific aspect. A good agreement with observations does not constitute final evidence that models are correct, but a consistently bad agreement with observations clearly indicates some problems of the models[34]. Different approaches have been taken to reduce the model spread in projections of Arctic sea-ice area for a given emission scenario. One such approach consists in giving a weight to each model based on its performance relative to observations during the historical period: models that strongly agree with observations receive more weight than models that poorly agree[31,34,35]. Another approach is to select models based on their historical performance and exclude models that do not satisfy the selection criteria[21,24,36,37].

In our study, we adopt the latter approach, i.e. model selection, as it allows to exclude model outliers that show large biases in relevant variables for Arctic sea-ice representation based on clearly defined selection criteria. We define a series of selection criteria based on the mean, variability and trend in Arctic sea-ice area and volume (see 'Methods' section and Supplementary Table 1). The northward Atlantic and Pacific ocean heat transports at different latitudes are also used as selection criteria as they have been shown to have a large influence on recent sea-ice changes[29,30,38–40]. While the atmosphere drives most Arctic sea-ice loss in the short term (within a decade), the ocean plays a greater role in the long term (beyond 10 years)[41]. These criteria are used to retain CMIP6 models closest to observations over the historical period (1979–2014), and allow us to compute the multi-model mean Arctic sea-ice area and volume until the end of the twenty-first century based on the selected models, thus refining model projections of Arctic sea-ice area and volume. To reduce the effect of internal variability, we use the longest possible period for the model—observation comparison and use all existing ensemble members[16,33].

Projections with model selection. When applying our selection criteria, we find that the Arctic sea-ice area and volume generally reach lower values at the end of this century compared to the case without selection, for both emission scenarios (Figs. 2 and 3 and Supplementary Figs. 1 and 3–5), in agreement with a previous study using CMIP5 models[35]. This is mainly due to stronger
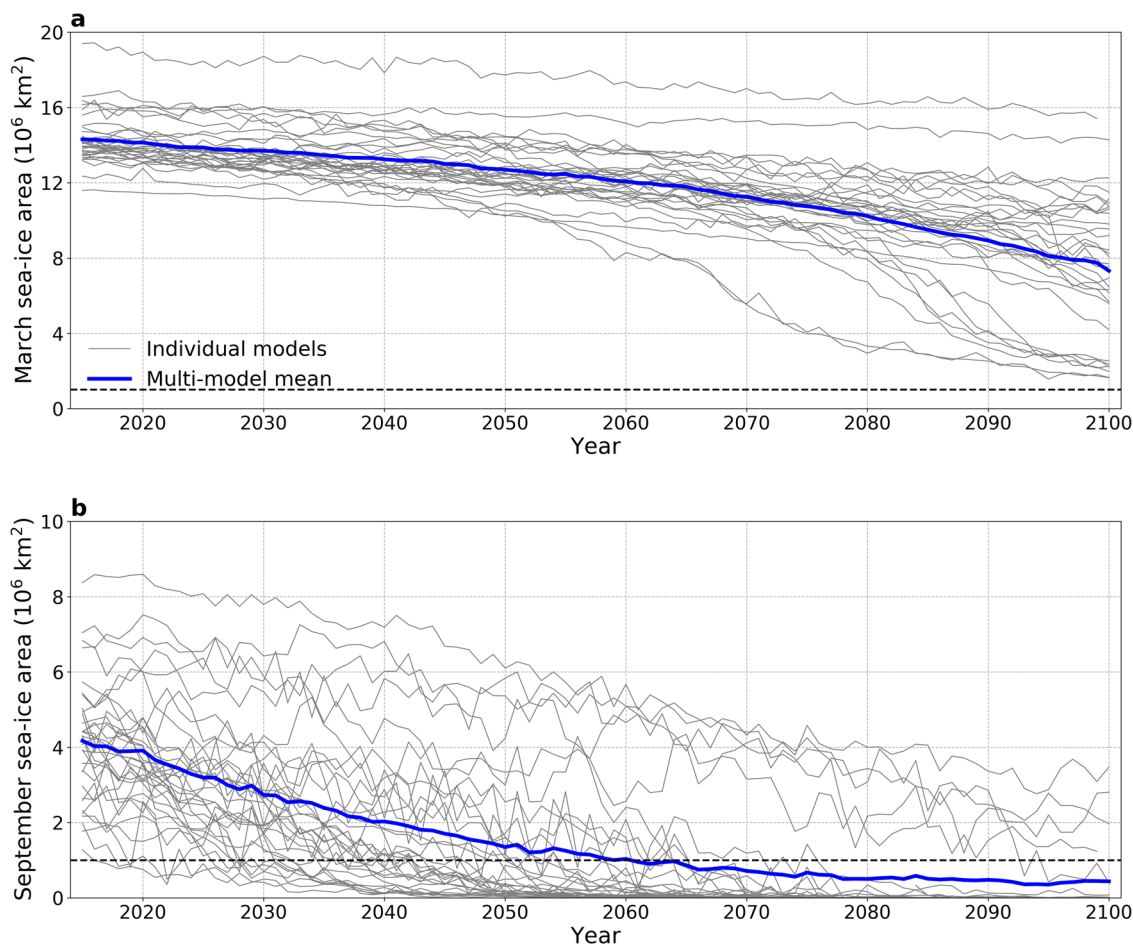
Fig. 1 Time evolution of future Arctic sea-ice area in CMIP6 models. Time evolution is provided for individual model ensemble means (thin grey curves) and the multi-model mean (thick blue curve). **a** March and (**b**) September Arctic sea-ice area based on the SSP5-8.5 scenario. The horizontal dashed line represents the ice-free Arctic threshold.

reductions in sea-ice area and volume over the twenty-first century in the selected models, and to a lesser extent due to smaller initial present-day Arctic sea-ice area (Fig. 3 and Supplementary Fig. 5). The stronger reductions in sea-ice area and volume over the twenty-first century partly stem from the fact that some of the selected models have a larger sensitivity to anthropogenic global warming than the non-selected models. Also, the smaller present-day sea-ice area in the selected models is due to the fact that the multi-model mean without selection overestimates the observed sea-ice area (Fig. 3a, b); thus, the selection of models closer to observations reduces this overestimation, explaining the smaller present-day sea-ice area. We checked the robustness of our results by performing a bootstrap analysis in which we randomly selected 10 models and averaged the results over 1000 realizations. As the multi-model mean sea-ice area and volume averaged over the random selection are very close to the multi-model mean over the full sample of models (Fig. 3), our finding that model selection with our criteria leads to smaller sea-ice area and volume is robust.

The loss of sea-ice area and volume over this century is most pronounced when selecting models that best represent the historical Atlantic and Pacific ocean heat transports, in combination or not with the mean sea-ice area and volume (Figs. 2 and 3 and Supplementary Figs. 1 and 3–5). In the high-emission scenario and for all selection criteria including ocean heat transport, March sea-ice area and volume reach less than 7 million km^2 and less than 5000 km^3, respectively, by the end

of the twenty-first century, and September sea ice completely disappears (Fig. 3). Selecting models that best represent the observed mean sea-ice area and volume and trend in sea-ice area also provides a stronger reduction in future Arctic sea-ice area and volume compared to no selection, especially in September, but that reduction is less strong than with the ocean heat transport criteria (Figs. 2 and 3 and Supplementary Figs. 1 and 3–5).

The selections based on the variability in sea-ice area and volume and trend in sea-ice volume are not as clear-cut: depending on the month or the scenario, these selection criteria provide smaller or larger reductions in sea-ice area and volume (Figs. 2 and 3 and Supplementary Figs. 1 and 3–5). For sea-ice area and volume variability, this is partly linked to the fact that these quantities are directly related to atmospheric variability[10]. In turn, the latter does not highly depend on the total amount of ice. Thus, even a model with too much (or not enough) sea ice can have a realistic atmospheric variability, leading to a realistic sea-ice variability.

An additional model selection criterion that we include in our analysis is the minimum number of ensemble members. We select all models that have at least five members, as this allows to both keep models that partly take into account the uncertainty linked to internal variability and to have about a third of the total number of models (ten models). We find that the multi-model mean averaged over these models also leads to a stronger sea-ice loss relative to no selection, with no remaining sea ice in September by the end of the century and reductions of 60% and
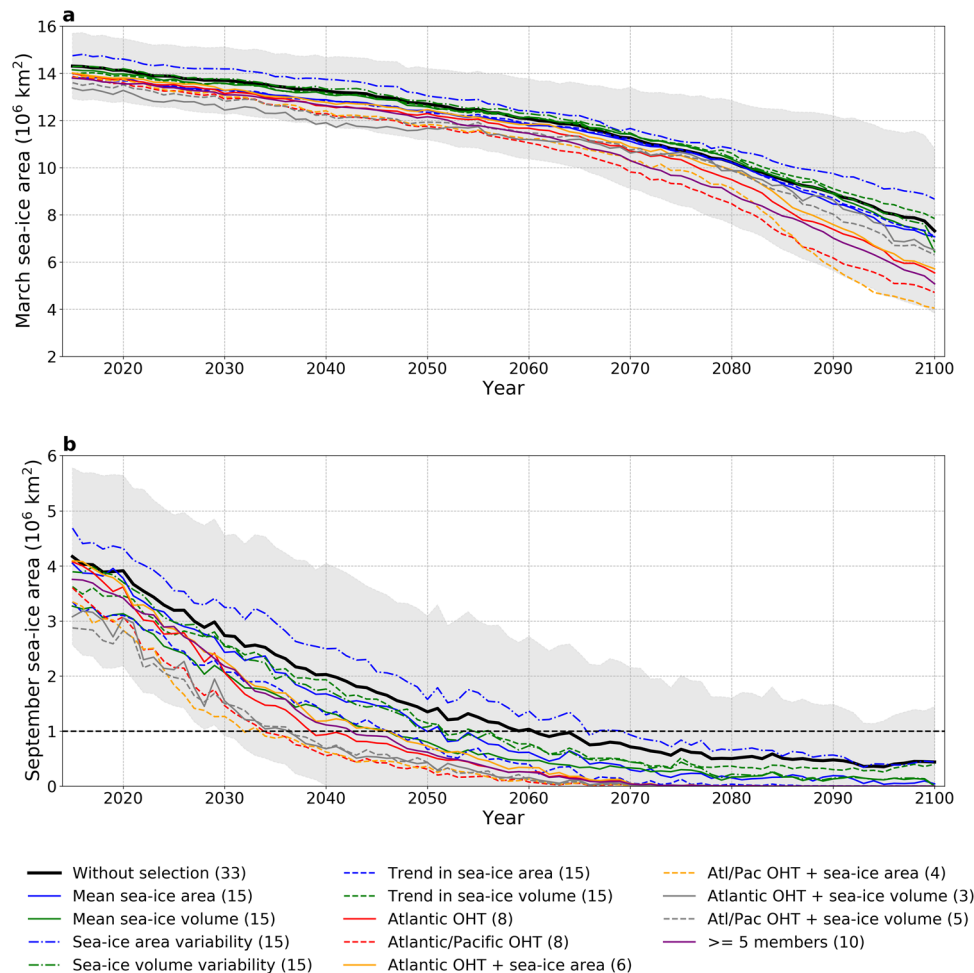
Fig. 2 Time evolution of future Arctic sea-ice area according to different selection criteria. Time evolution is provided for the CMIP6 multi-model mean averaged over all models (thick black curve) and averaged over the models selected according to different criteria (coloured curves). **a** March and (**b**) September Arctic sea-ice area based on the SSP5-8.5 scenario. The light grey shading shows the standard deviation around the multi-model mean without selection. The number of models included in each multi-model average is indicated in parenthesis in the legend. The horizontal dashed line represents the ice-free Arctic threshold.

87% in March sea-ice area and volume, respectively, in the high-emission scenario (Figs. 2 and 3). It is important to point out that seven models (out of ten) selected according to the number of members are also selected in at least another selection criterion associated with ocean heat transport (Supplementary Table 1). The three remaining models are also selected in criteria related to mean sea-ice area, mean sea-ice volume and/or trend in sea-ice area. Thus, the models selected according to the number of members tend to be the ones that are also selected in criteria presenting a larger sea-ice loss compared to the multi-model mean without selection.

Ice-free Arctic. Our model selection based on historical performance allows to exclude outliers that have either too much or not enough Arctic sea ice. For the winter months, outliers are mainly located on the high end as most models overestimate the observed sea-ice area (Fig. 3a), while for the summer months outliers are located on either end (Fig. 3b)[24]. Thus, our model selection narrows down the spread in model projections of Arctic sea ice by excluding outliers. In particular, the threshold of an ice-free Arctic in summer is reached earlier with model selection compared to without selection. In the high-emission scenario, five out of six selection criteria that include ocean heat transport provide a

first ice-free Arctic in September before 2040 (range of multi-model means: 2032–2039), more than 20 years before the date of ice-free Arctic for the multi-model mean without model selection (i.e. 2061) (Fig. 4). In the selection based on the number of members, the first September ice-free Arctic is reached in 2043. The selection criteria associated with only sea-ice area or volume provide a later date of ice-free Arctic, but still about a decade before the case without selection (between 2047 and 2052), except for the selection based on sea-ice area variability (2066) (Fig. 4). These results are in agreement with a previous study[35] in which a multiple diagnostic ensemble regression is applied to CMIP5 models using model weights. They also find an earlier near-disappearance of Arctic sea ice by more than a decade in the high-emission scenario.

It is important to point out that in the high-emission scenario four models do not reach ice-free conditions in September before the end of the twenty-first century and have a relatively large sea-ice area compared to other models (Fig. 1b). This explains the relatively late date of first ice-free Arctic for multi-model means that include these models, i.e. without selection and associated with four selection criteria (mean sea-ice volume, sea-ice area variability, sea-ice volume variability and trend in sea-ice volume), compared to the spread in first ice-free Arctic date of models included in these criteria (Fig. 4). In particular, the year of
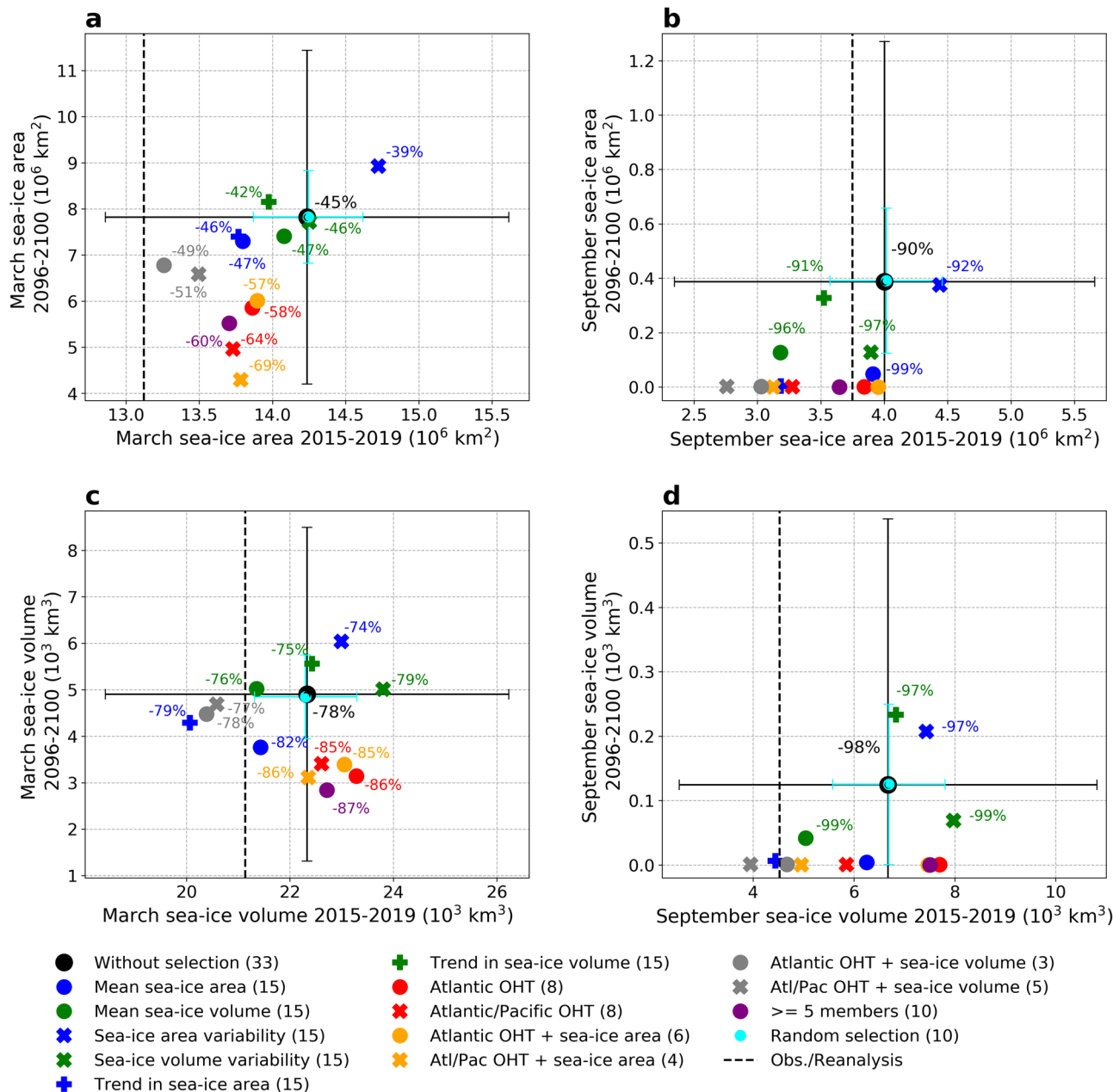
Fig. 3 Arctic sea-ice area and volume in 2096–2100 against 2015–2019. Quantities are provided for the CMIP6 multi-model mean averaged over all models (black dot, with the ensemble standard deviation as error bars), the multi-model mean averaged over a 10-model random selection (cyan dot with the corresponding error bars for 1000 realizations) and the multi-model means averaged over the models selected according to different criteria (coloured dots and crosses), based on the SSP5-8.5 scenario. **a** March Arctic sea-ice area, **b** September Arctic sea-ice area, **c** March Arctic sea-ice volume, **d** September Arctic sea-ice volume. The relative change in sea-ice area/volume between 2015 and 2019 and 2096 and 2100 is shown beside the different items (not indicated if the change is −100%). The dashed vertical lines show (**a**, **b**) the sea-ice area from OSI SAF observations and (**c**, **d**) sea-ice volume from PIOMAS reanalysis in 2015–2019. The number of models included in each multi-model average is indicated in parenthesis in the legend.

first ice-free Arctic is 2061 for the multi-model mean averaged over all models, while a majority of models (64%) reach this threshold before 2050. If we remove the four models that do not reach ice-free conditions before 2100, the multi-model mean first ice-free Arctic date is advanced to 2048, and is within the range of selection criteria based on sea-ice area and volume only. As our different model selections generally exclude the four models that do not reach ice-free conditions before 2100, the timing of ice-free conditions occurs earlier compared to the multi-model mean without selection.

In the low-emission scenario, the six selection criteria that include ocean heat transport and the five-member selection

criterion all provide a first ice-free Arctic in September at least some years before the end of this century, but with a sea-ice area staying close to the 1 million km² threshold until the end of the century (Supplementary Figs. 4b and 6). For five out of six criteria that include ocean heat transport, the date of first ice-free Arctic is delayed by 4–16 years compared to the high-emission scenario, while it is delayed by 33 years for the selection based on the number of members and 36 years for the remaining ocean heat transport criterion. Ice-free conditions are also reached in the last decade of the twenty-first century for the multi-model mean based on the trend in sea-ice area (46 years later than in the high-emission scenario). For the five remaining selection criteria based
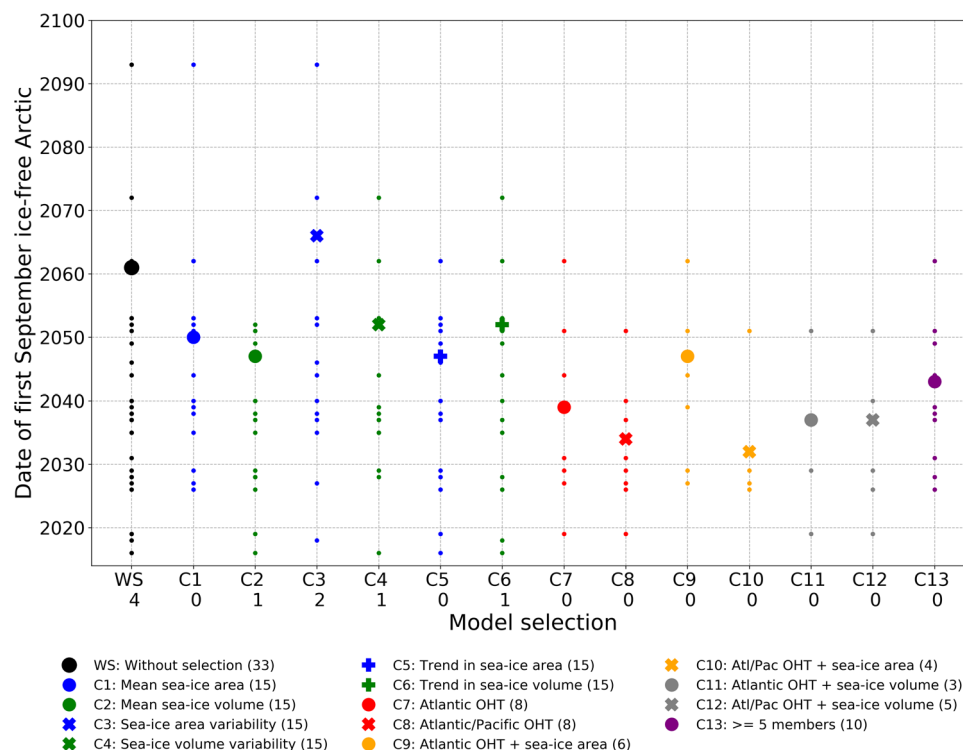
Fig. 4 Date of first September ice-free Arctic. The date of first ice-free Arctic is defined as the year when September sea-ice area drops below 1 million km^2 for the first time, for the different selection criteria (C1–C13) and without selection (WS), based on the SSP5-8.5 scenario. The big symbols show the dates of the multi-model means, while the small dots show the dates of the models included in each criterion. The number of models that do not reach ice-free conditions before the end of the century is indicated below X labels. The number of models included in each multi-model average is indicated in parenthesis in the legend.

only on sea-ice area or volume, ice-free conditions are not reached before 2100 in the low-emission scenario (Supplementary Fig. 6). In addition, although 45% of the models simulate an ice-free Arctic before 2050, no ice-free Arctic occurs in this century for the multi-model mean averaged over all models, as 12 models do not reach ice-free conditions before 2100 (Supplementary Fig. 6).

Conclusions. The rapid ongoing disintegration of Arctic sea ice can have dramatic consequences on other components of the climate system, such as the atmosphere[42,43] and the ocean[44,45], as well as the biosphere and our societies[1]. This calls for a need to improve the future projections of Arctic sea ice. In our study, we have shown that these projections can potentially be improved by selecting climate models that best represent the present state in terms of sea-ice area, sea-ice volume and northward ocean heat transport. This model selection reveals that sea-ice area and volume reach lower values at the end of this century compared to the multi-model mean without selection. This arises both from a more rapid reduction in these quantities through this century and from a lower present-day sea-ice area. Using such a model selection, the timing of an almost ice-free Arctic in summer is advanced by up to 29 years in the high-emission scenario, i.e. it could occur as early as around 2035. Thus, these results highlight a potential underestimation of the future Arctic sea-ice loss when including all CMIP6 models.

Another way to reduce uncertainties in future model projections of Arctic sea ice is to extend our methodology to process-based selection criteria. In our study, we found that the selection criteria related to ocean heat transport, known to be a key driver of the recent sea-ice loss, provide the earliest dates of a first ice-free Arctic. Identifying the models that are able to correctly reproduce the mechanisms by which sea ice is affected by ocean heat transport (and other climate drivers) would allow to provide better future projections of Arctic sea ice.

Methods

CMIP6 model simulations. In our study, we analysed outputs from climate models participating in the CMIP6 effort[27]. We extracted the monthly mean sea-ice concentration and sea-ice volume per area (or sea-ice thickness if the sea-ice volume per area was not available) from CMIP6 models that were run over both the historical period (1850–2014) and the future (2015–2100), using SSP1-2.6 (weak greenhouse gas emission scenario) and SSP5-8.5 (strong greenhouse gas emission scenario). We computed the total Arctic sea-ice area as the product of sea-ice concentration and grid-cell area summed over the ocean region north of 40°N. The total Arctic sea-ice volume is the product of sea-ice volume per area (or sea-ice thickness times sea-ice concentration) and grid-cell area summed over the ocean region north of 40°N. Sea-ice area from 32 models is used for the SSP1-2.6 scenario and from 33 models for the SSP5-8.5 scenario (Supplementary Table 1). As some models have run several ensemble members with different initial conditions, we have a total of 166 model simulations for both SSP1-2.6 and SSP5-8.5. Sea-ice volume from 28 models is used for both SSP1-2.6 and SSP5-8.5, including a total of 155 member simulations for SSP1-2.6 and 154 member simulations for SSP5-8.5. In addition, we extracted the monthly mean historical northward ocean heat transport (computed directly by the different models) from 16 models (it was not available for the other models). We computed the ensemble mean sea-ice area, sea-ice volume and ocean heat transport over all members for each individual model. In our study, we always use the ensemble mean for each individual model, as we think it provides the best representation of the response to an increase in greenhouse gas emissions. Supplementary Table 1 provides the number of ensemble members available for each model and each variable. References of the model simulations used in our study are provided in Supplementary Tables 2–4.

Reference products. In order to evaluate CMIP6 models over the historical period, we used different observational and reanalysis datasets. For sea-ice area, we retrieved sea-ice concentration from the European Organisation for the Exploitation of Meteorological Satellites (EUMETSAT) Ocean Sea Ice Satellite Application Facility (OSI SAF)[46] available since 1979, and we integrated this quantity over the northern hemisphere (north of 40°N). We used sea-ice volume from the Pan-Arctic

Ice-Ocean Modelling and Assimilation System (PIOMAS)[6], which is a coupled ocean—sea ice model with capability of assimilating daily sea-ice concentration and sea-surface temperature. This dataset is available since 1979 and shows reasonable agreement with observations[47]. Estimates of ocean meridional heat transport (Atlantic and Pacific) come from Trenberth et al.[48] and are deduced from top-of-atmosphere radiation coming from Clouds and the Earth's Radiant Energy System, vertically integrated atmospheric energy divergence from ERA-Interim, and ocean heat content from Ocean Reanalysis System 5. This dataset is available for the period 2000–2016. Finally, we also used Atlantic Ocean heat transport estimates derived from the Rapid Climate Change Meridional Overturning Circulation and Heatflux Array (RAPID-MOCHA) observing system deployed at 26°N (2004–2018)[49], as well as from the Overturning in the Subpolar North Atlantic Programme (OSNAP) observing system deployed around 57°N (2014 and 2016)[50].

Selection criteria. In order to retain CMIP6 models closest to observations and reanalysis over the historical period, we defined a series of selection criteria based on sea-ice area, sea-ice volume, ocean heat transport and the number of ensemble members. Here is a description of these selection criteria:

(1) Mean sea-ice area: we selected the 15 models (about half of the available models) closest to the observed mean sea-ice area averaged over 1979–2014 for both March and September combined.
(2) Mean sea-ice volume: same as criterion 1 for sea-ice volume.
(3) Sea-ice area variability: we selected the 15 models closest to the observed detrended standard deviation in sea-ice area over 1979–2014 for both March and September combined.
(4) Sea-ice volume variability: same as criterion 3 for sea-ice volume.
(5) Trend in sea-ice area: we selected the 15 models closest to the observed trend in sea-ice area over 1979–2014 for both March and September combined.
(6) Trend in sea-ice volume: same as criterion 5 for sea-ice volume.
(7) Atlantic ocean heat transport ('Atlantic OHT' in the figure legends): we selected the eight models (half of the models having ocean heat transport) closest to the observed mean Atlantic ocean heat transport at both 26°N and 57°N combined, averaged over 2000–2014. As the OSNAP measurements at 57°N only cover 2014 and 2016, we used the mean of these 2 years for the observed mean value at this latitude.
(8) Atlantic and Pacific ocean heat transports ('Atl/Pac OHT' in the figure legends): we selected the eight models closest to the observed mean ocean heat transport at both 70°N in the Atlantic Ocean and 60°N in the Pacific Ocean (combined), averaged over 2000–2014.
(9) Atlantic ocean heat transport and mean sea-ice area ('Atlantic OHT + sea-ice area' in the figure legends): we selected the six models included in both criteria 7 and 1.
(10) Atlantic and Pacific ocean heat transports and mean sea-ice area ('Atl/Pac OHT + sea-ice area' in the figure legends): we selected the four models included in both criteria 8 and 1.
(11) Atlantic ocean heat transport and mean sea-ice volume ('Atlantic OHT + sea-ice volume' in the figure legends): we selected the three models included in both criteria 7 and 2.
(12) Atlantic and Pacific ocean heat transports and mean sea-ice volume ('Atl/Pac OHT + sea-ice volume' in the figure legends): we selected the five models included in both criteria 8 and 2.
(13) Number of ensemble members ('≥5 members' in the figure legends): we retained only the models that have at least five ensemble members in the projection scenarios (ten models in total).

For criteria 1–8, we combined March and September sea-ice quantities (criteria 1–6), Atlantic ocean heat transport at two latitudes (criterion 7) and Atlantic and Pacific ocean heat transports (criterion 8). For these criteria, we looked at the ranking of the two diagnostics (e.g. March and September mean sea-ice area for criterion 1) and we picked models that are best placed in the two rankings combined until we selected the desired amount of models (e.g. 15 models for criterion 1). The models that are included in each selection criterion are shown in Supplementary Table 1. For each selection criterion, we computed the multi-model mean sea-ice area and volume (Figs. 2 and 3 and Supplementary Figs. 1 and 3–5).

As each model selection reduces the number of models taken into account for computing the associated multi-model mean, we also performed a bootstrap analysis in which we randomly selected ten models and we averaged the results over 1000 realizations (Fig. 3 and Supplementary Fig. 5, in which the error bars show the standard deviations over the 1000 realizations). This allows to check that our results obtained with our selection criteria are not obtained by chance.

Data availability
All the CMIP6 model data[27] used in this study (historical and scenario runs) can be accessed through the ESGF nodes: https://esgf-node.llnl.gov/search/cmip6. A list of the model simulations used in this study and associated references is provided in Supplementary Tables 2–4. The observed sea-ice concentration from OSI SAF[46] can be accessed through the EUMETSAT repository: https://doi.org/10.15770/EUM_SAF_OSI_0008. The PIOMAS[6] sea-ice volume data can be accessed via the Polar

Science Center of the University of Washington: http://psc.apl.uw.edu/research/projects/arctic-sea-ice-volume-anomaly. The ocean meridional heat transport estimates from Trenberth et al.[48] are located here: https://doi.org/10.5065/9v3y-fn61. The RAPID-MOCHA[49] ocean heat transport at 26.5°N can be retrieved from the Rosenstiel School Ocean Technology Lab: https://mocha.rsmas.miami.edu/mocha/results/index.html. The OSNAP[50] ocean heat transport data can be accessed here: https://www.o-snap.org/observations/data.

Code availability
The Python scripts to produce the figures of this article are available on Zenodo: https://zenodo.org/record/4912115.

References
1. IPCC. *Summary for Policymakers.* In *IPCC Special Report on the Ocean and Cryosphere in a Changing Climate* (eds Pörtner, H.-O., et al.) (Cambridge University Press, Cambridge, United Kingdom and New York, NY, USA, 2019).
2. Onarheim, I. H., Eldevik, T., Smedsrud, L. H. & Stroeve, J. C. Seasonal and regional manifestation of Arctic sea ice loss. *J. Clim.* **31**, 4917–4932 (2018).
3. Stroeve, J. & Notz, D. Changing state of Arctic sea ice across all seasons. *Environ. Res. Lett.* **13**, 103001 (2018).
4. Lindsay, R. & Schweiger, A. Arctic sea ice thickness loss determined using subsurface, aircraft, and satellite observations. *The Cryosphere* **9**, 269–283 (2015).
5. Kwok, R. Arctic sea ice thickness, volume, and multiyear ice coverage: losses and coupled variability (1958-2018). *Environ. Res. Lett.* **13**, 105005 (2018).
6. Zhang, J. & Rothrock, D. A. Modeling global sea ice with a thickness and enthalpy distribution model in generalized curvilinear coordinates. *Monthly Weather Rev.* **131**, 845–861 (2003).
7. Schweiger, A., Wood, K. R. & Zhang, J. Arctic sea ice volume variability over 1901-2010: A model-based reconstruction. *J. Clim.* **32**, 4731–4752 (2019).
8. Mahlstein, I. & Knutti, R. September Arctic sea ice predicted to disappear for 2°C global warming above present. *J. Geophys. Res.* **117**, D06104 (2012).
9. Niederdrenk, A. L. & Notz, D. Arctic sea ice in a 1.5 °C warmer world. *Geophys. Res. Lett.* **45**, 1963–1971 (2018).
10. Olonscheck, D., Mauritsen, T. & Notz, D. Arctic sea-ice variability is primarily driven by atmospheric temperature fluctuations. *Nat. Geosci.* **12**, 430–434 (2019).
11. Notz, D. & Stroeve, J. Observed Arctic sea-ice loss directly follows anthropogenic CO_2 emission. *Science* **354**, 747–750 (2016).
12. Andry, O., Bintanja, R. & Hazeleger, W. Time-dependent variations in the Arctic's surface albedo feedback and the link to seasonality in sea ice. *J. Clim.* **30**, 393–410 (2017).
13. Goosse, H. et al. Quantifying climate feedbacks in polar regions. *Nat. Commun.* **9**, 1–13 (2018).
14. Notz, D. & Stroeve, J. The trajectory towards a seasonally ice-free Arctic Ocean. *Curr. Clim. Change Rep.* **4**, 407–416 (2018).
15. Simmonds, I. & Rudeva, I. The great Arctic cyclone of August 2012. *Geophys. Res. Lett.* **39**, L23709 (2012).
16. Swart, N. C., Fyfe, J. C., Hawkins, E., Kay, J. E. & Jahn, A. Influence of internal variability on Arctic sea-ice trends. *Nat. Clim. Change* **5**, 86–89 (2015).
17. Ding, Q. et al. Influence of high-latitude atmospheric circulation changes on summertime Arctic sea ice. *Nat. Clim. Change* **7**, 289–295 (2017).
18. England, M., Jahn, A. & Polvani, L. Non-uniform contribution of internal variability to recent Arctic sea ice loss. *J. Clim.* **32**, 4039–4053 (2019).
19. Jahn, A., Kay, J. E., Holland, M. M. & Hall, D. M. How predictable is the timing of a summer ice-free Arctic? *Geophys. Res. Lett.* **43**, 9113–9120 (2016).
20. Screen, J. A. & Deser, C. Pacific Ocean variability influences the time of emergence of a seasonally ice-free Arctic Ocean. *Geophys. Res. Lett.* **46**, 2222–2231 (2019).
21. Massonnet, F. et al. Constraining projections of summer Arctic sea ice. *The Cryosphere* **6**, 1383–1394 (2012).
22. Rosenblum, E. & Eisenman, I. Sea ice trends in climate models only accurate in runs with biased global warming. *J. Clim.* **30**, 6265–6278 (2017).
23. Davy, R. & Outten, S. The Arctic surface climate in CMIP6: Status and developments since CMIP5. *J. Clim.* **33**, 8047–8068 (2020).
24. SIMIP Community. Arctic sea ice in CMIP6. *Geophys. Res. Lett.* **47**, e2019GL086749 (2020).
25. Meehl, G. A. et al. The WCRP CMIP3 multimodel dataset. *Bull. Am. Meteorological Soc.* **88**, 1383–1394 (2007).

26. Taylor, K. E., Stouffer, R. J. & Meehl, G. A. An overview of CMIP5 and the experiment design. *Bull. Am. Meteorological Soc.* **93**, 485–498 (2012).

27. Eyring, V. et al. Overview of the Coupled Model Intercomparison Project Phase 6 (CMIP6) experimental design and organization. *Geosci. Model Dev.* **9**, 1937–1958 (2016).

28. O'Neill, B. C. et al. The Scenario Model Intercomparison Project (ScenarioMIP) for CMIP6. *Geosci. Model Dev.* **9**, 3461–3482 (2016).

29. Arthun, M., Eldevik, T., Smedsrud, L. H., Skagseth, O. & Ingvaldsen, R. B. Quantifying the influence of Atlantic heat on Barents Sea ice variability and retreat. *J. Clim.* **25**, 4736–4743 (2012).

30. Polyakov, I. V. et al. Greater role for Atlantic inflows on sea-ice loss in the Eurasian Basin of the Arctic Ocean. *Science* **356**, 285–291 (2017).

31. Brunner, L. et al. Reduced global warming from CMIP6 projections when weighting models by performance and independence. *Earth Syst. Dynamics* **11**, 995–1012 (2020).

32. Hawkins, E. & Sutton, R. The potential to narrow uncertainty in regional climate predictions. *Bull. Am. Meteorological Soc.* **90**, 1095–1107 (2009).

33. Bonan, D. B., Lehner, F. & Holland, M. M. Partitioning uncertainty in projections of Arctic sea ice. *Environ. Res. Lett.* **16**, 044002 (2021).

34. Knutti, R. et al. A climate model projection weighting scheme accounting for performance and interdependence. *Geophys. Res. Lett.* **44**, 1909–1918 (2017).

35. Senftleben, D., Lauer, A. & Karpechko, A. Constraining uncertainties in CMIP5 projections of September Arctic sea ice extent with observations. *J. Clim.* **33**, 1487–1503 (2020).

36. Wang, M. & Overland, J. E. A sea ice free summer Arctic within 30 years: An update from CMIP5 models. *Geophys. Res. Lett.* **39**, L18501 (2012).

37. Liu, J., Song, M., Horton, R. M. & Hu, Y. Reducing spread in climate model projections of a September ice-free Arctic. *Proc. Natl Acad. Sci.* **110**, 12571–12576 (2013).

38. Holland, M. M., Bitz, C. M. & Tremblay, B. Future abrupt reductions in the summer Arctic sea ice. *Geophys. Res. Lett.* **33**, L23503 (2006).

39. Serreze, M. C., Barrett, A. P., Crawford, A. D. & Woodgate, R. A. Monthly variability in Bering Strait oceanic volume and heat transports, links to atmospheric circulation and ocean temperature, and implications for sea ice conditions. *J. Geophys. Res.* **124**, 9317–9337 (2019).

40. Docquier, D., Koenigk, T., Fuentes-Franco, R., Karami, M. P. & Ruprich-Robert, Y. Impact of ocean heat transport on the Arctic sea-ice decline: a model study with EC-Earth3. *Clim. Dynamics* **56**, 1407–1432 (2021).

41. Garuba, O. A., Singh, H. A., Hunke, E. & Rasch, P. J. Disentangling the coupled atmosphere-ocean-ice interactions driving Arctic sea ice response to CO2 increases. *J. Adv. Modeling Earth Syst.* **12**, e2019MS001902 (2020).

42. Overland, J. E. & Wang, M. Large-scale atmospheric circulation changes are associated with the recent loss of Arctic sea ice. *Tellus A* **62**, 1–9 (2010).

43. Dai, A., Luo, D., Song, M. & Liu, J. Arctic amplification is caused by sea-ice loss under increasing CO2. *Nat. Commun.* **10**, 1–13 (2019).

44. Bhatt, U. S. et al. Implications of Arctic sea ice decline for the Earth System. *Ann. Rev. Environ. Res.* **39**, 57–89 (2014).

45. Sévellec, F., Fedorov, A. V. & Liu, W. Arctic sea-ice decline weakens the Atlantic Meridional Overturning Circulation. *Nat. Clim. Change* **7**, 604–610 (2017).

46. Lavergne, T. et al. Version 2 of the EUMETSAT OSI SAF and ESA CCI sea-ice concentration climate data records. *The Cryosphere* **13**, 49–78 (2019).

47. Schweiger, A. et al. Uncertainty in modeled Arctic sea ice volume. *J. Geophys. Res.* **116**, C00D06 (2011).

48. Trenberth, K. E., Zhang, Y., Fasullo, J. T. & Cheng, L. Observation-based estimates of global and basin ocean meridional heat transport time series. *J. Clim.* **32**, 4567–4583 (2019).

49. Johns, W. E. et al. Continuous, array-based estimates of Atlantic Ocean heat transport at 26.5N. *J. Clim.* **24**, 2429–2449 (2011).

50. Lozier, M. S. et al. A sea change in our view of overturning in the subpolar North Atlantic. *Science* **363**, 516–521 (2019).

Acknowledgements

Author contributions

D.D. led the work with contributions from T.K. D.D. performed the computations, analysed the results, produced the figures and led the paper writing. T.K. participated in the design of the study, the interpretation of the results and the writing of the paper.

Competing interests

The authors declare no competing interests

Additional information

Supplementary information The online version contains supplementary material available at https://doi.org/10.1038/s43247-021-00214-7.

Correspondence and requests for materials should be addressed to D.D.

Peer review information Communications Earth & Environment thanks Patricia DeRepentigny and the other, anonymous, reviewers for their contribution to the peer review of this work. Primary Handling Editors: Jan Lenaerts, Joe Aslin. Peer reviewer reports are available.

Reprints and permission information is available at http://www.nature.com/reprints

Publisher's note Springer Nature remains neutral with regard to jurisdictional claims in published maps and institutional affiliations.